# Surface-enhanced Raman spectroscopy with gold nanoparticle dimers created by sacrificial DNA origami technique

*Naoki Yamashita*[1] ✉, *Seongsu Park*[1], *Kentaro Kawai*[2], *Yoshikazu Hirai*[1], *Toshiyuki Tsuchiya*[1], *Osamu Tabata*[1]

[1]*Department of Microengineering, Graduate School of Engineering, Kyoto University, Kyoto, Japan*
[2]*Department of Precision Science and Technology, Graduate School of Engineering, Osaka University, Osaka, Japan*
✉ *E-mail: n_yamashita@nms.me.kyoto-u.ac.jp*

Published in Micro & Nano Letters; Received on 3rd July 2019; Revised on 27th December 2019; Accepted on 5th February 2020

In a previously proposed method for molecular detection based on surface-enhanced Raman spectroscopy (SERS), gold nanoparticle (AuNP) dimers are formed on a substrate using DNA origami with a nanometre-scale gap between them. In this sacrificial DNA origami technique, a conjugate of two AuNPs and a DNA origami is deposited on a silicon chip, and then the DNA origami is selectively removed using vacuum ultraviolet light and ultrapure water rinsing to form surface-clean AuNP dimers. The performance of SERS-based molecular detection of AuNP dimers created using the proposed technique with a 30 nm AuNP diameter has now been evaluated. The Raman signals from the target molecules (4,4′-bipyridine) were greatly enhanced and thus successfully detected.

**1. Introduction:** Surface-enhanced Raman spectroscopy (SERS) is a practical analysis method for detecting and identifying molecules dissolved in water at low concentration [1–3]. It is thus attracting interest in various fields, including medicine, biology, and environmental monitoring. In SERS, a metallic nanostructure with nanometre-scale gaps (nanogaps) is required to generate a strong electric field and enhance the Raman scattered light [4–8]. However, creating metal nanostructures with nanogaps from thin metal film using a lift-off process is not easy due to the resolution limit of electron beam lithography and the difficulty of controlling crystal growth of metal nanostructures [6–8]. An alternative method using gold nanoparticles (AuNPs) synthesised in solution with a controlled size and arranged on a substrate has thus been developed [1–3, 9, 10]. In this method, two AuNPs covered by a citrate molecular layer for stabilisation in solution are trapped in a nanometre-scale groove created using a nanofabrication technique such as electron beam lithography. The molecular layers between the two AuNPs are removed by UV/$O_3$ cleaning, resulting in the formation of a nanogap between them [1]. Such AuNP dimers enhance the Raman signals of the molecules trapped in the nanogaps due to the strong electric field. However, fabricating such AuNP dimers with this method is costly due to the use of electron beam lithography.

In a newer low-cost approach to high-sensitivity SERS analysis, DNA origami are used to form AuNP dimers [10–16]. A DNA origami is a nanostructure formed by self-assembly of short single-stranded DNAs (ssDNAs), called staple strands, onto a scaffold strand, which is a long circular ssDNA [17]. The size of DNA origami folding a scaffold into the designed shape is typically less than $100 \times 100$ nm square, and its thickness is about 2 nm, corresponding to the diameter of a double-stranded DNA (dsDNA) segment. Extending an ssDNA from a staple strand, which is not hybridised with a scaffold strand, enables it to work as a connector and hybridise with a complementary ssDNA fixed on an AuNP. Therefore, a DNA origami can arrange AuNPs in its structure. This characteristic of DNA origami has been used in several studies on connecting two AuNPs to the counter-face of a DNA origami to create a pair of AuNPs. The separation between each AuNP in the pair corresponds to the thickness of the DNA origami [15, 16]. Single-molecular SERS analyses were performed using a fluorescent molecule intentionally fixed in the nanogap between the AuNPs in pair [13–16].

However, there has been no research on the application of AuNP dimers formed by DNA origami to the molecular trace analysis of molecules dissolved in water, since the target molecules cannot approach the nanogaps due to the DNA origami and connector strands between the two AuNPs. Moreover, these DNAs segment also generate SERS signals as a noise in the SERS analysis.

In our previous study, we devised a 'sacrificial DNA origami technique' for forming AuNP dimers with nanogaps by decomposing DNA origami using vacuum ultraviolet (VUV) light irradiation [18]. The AuNPs with a diameter of 15 nm were connected to the counter-faces of a rectangular DNA origami structure, and then the DNA origami was removed with a cleaning process using VUV irradiation and an ultrapure water (UPW) rinse. Finally, surface-clean AuNP dimers with an average gap of 1.5 nm were formed on a Si chip.

In the study reported here, AuNPs with a diameter of 30 nm, which exhibited sufficient enhancement of the electrical field for SERS analysis, were connected to newly designed DNA origami, and the dimer yields were evaluated by field emission scanning electron microscopy (FE-SEM) observation. The conjugates, consisting of two AuNPs and a DNA origami, were deposited onto the Si chip randomly, and then the DNA origami was selectively removed to form surface-clean AuNP dimers. The states of decomposing DNA origami between AuNP pairs were checked by SERS analysis in air after each step in the cleaning process used in the sacrificial DNA origami technique. Subsequently, molecular trace analysis for 4,4′-bipyridine dissolved in water at concentrations of 1 mM and 1 µM was conducted to evaluate the sensitivity of the SERS analysis.

**2. Materials and methods:** The schematic process flow for AuNP dimer preparation and SERS analysis is shown in Fig. 1 and explained as follows. The details of the experimental procedure were previously reported [18].

2.1. Preparing ssDNA functionalised AuNP (ssDNA–AuNP): First, 1.0 ml of a 0.33 nM colloidal solution containing 30 nm AuNPs (EMGC30; BBI Solutions) and 10 µl of 100 µM aqueous solution of thiol-terminated ssDNA (5′-HS-$C_6H_{12}$-TTT TTT TTT TTT TTT TTT TTT TTT TTT-3′; Eurofins Genomics) were mixed at a ratio of 1:3000. The AuNPs were covered with ssDNAs by salt ageing in Tris-borate-EDTA (TBE) buffer




doi: 10.1049/mnl.2019.0416

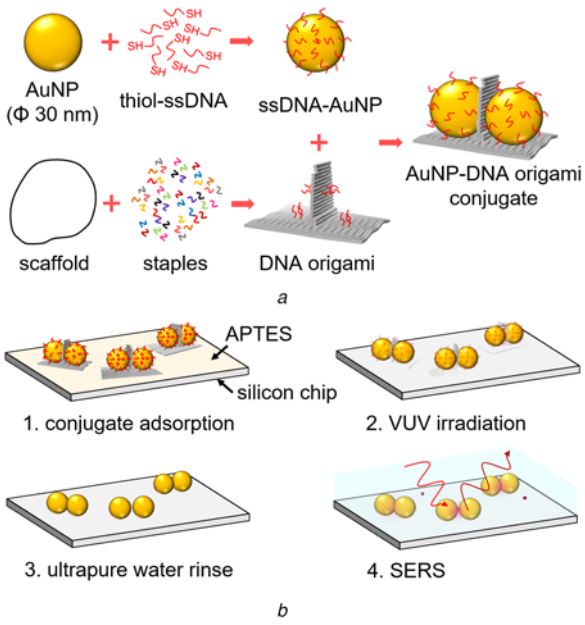


**Fig. 1** *Schematic illustration of experimental procedure*
*a* AuNP-DNA origami conjugate preparation
*b* SERS analysis

(1 M Tris, 0.9 M boric acid, and 0.01 M EDTA; Invitrogen), and the final NaCl concentration was set to 0.5 M. After 24 h incubation at room temperature, the excess thiol-terminated ssDNAs, which prevent connecting ssDNA–AuNPs to DNA origami, were removed by filtering with a centrifugal filter unit (Amicon Ultra 0.5 ml, NMWL 100 kDa; Merck Millipore). The filtering process was repeated eight times with 400 µl of 1 × Tris-EDTA (TE) buffer (5 mM Tris, 1 mM EDTA) by 10,000 rcf for 5 min at 4°C. The ssDNA–AuNPs were recovered by centrifuging at 1000 rcf for 5 min at 4°C.

2.2. Designing and folding DNA origami: A single-layer DNA origami, consisting of a partition and a vertically intersecting base part, was designed using open-source computer-aided design software caDNAno, and structure images were obtained by CanDo simulation. Three types of DNA origami with differently installed connector strands were designed to evaluate the AuNP dimer yield by exchanging three or six staples at each connecting point for staples with a 30-base extension of the poly-Adenine chains.

To fold the DNA origami, M13mp18 scaffold strands (N4040S; New England Biolabs) and 186 staple strands (Eurofins Genomics) were mixed in TE/Mg buffer (5 mM Tris, 1 mM EDTA, and 14 mM $MgCl_2$). The final concentrations of M13mp18, staples, and staples with connector strands in buffer were set at 5, 25, and 50 nM, respectively. This solution was prepared in a 100 µl batch, and its temperature was gradually reduced (from 90 to 80°C at −1°C/min; from 80 to 65°C at −0.5°C/min; from 65 to 25°C at −2°C/h). The excess staples and connector strands were removed using a centrifugal filter unit (Amicon Ultra 0.5 ml, NMWL 30 kDa; Merck Millipore). The filtering process was repeated eight times with 400 µl of 1 × TE buffer (5 mM Tris, 1 mM EDTA) containing 5 mM $MgCl_2$ by 5000 rcf for 5 min at 4°C. The DNA origami were recovered by centrifuging at 1000 rcf for 5 min at 4°C.

2.3. Creating AuNP–DNA origami conjugate and purification: After filtration in process I and II, the concentrations of ssDNA–AuNP and DNA origami in each solution were calculated with a UV/visible spectrophotometer (NanoDrop One; Thermo Scientific). Both solutions were then mixed in TE buffer containing 12 mM $MgCl_2$ and 300 mM NaCl. The final concentrations of DNA origami and ssDNA–AuNP were set at 2.5 and 15 nM. The mixture was annealed at 45 to 25°C (from 25 to 45°C for 10 min, and from 45 to 25°C for 50 min) for ten cycles to form AuNP–DNA origami conjugates. Large amounts of excess of ssDNA–AuNPs and aggregate structure were removed from the AuNP–DNA origami conjugate solution by agarose gel electrophoresis. A 0.7% agarose gel with 0.5 × TBE buffer containing 6 mM $MgCl_2$ was prepared, and the AuNP–DNA origami conjugate solution with a loading buffer (6 × Loading Buffer Orange G; Nippon Gene) was applied to the well of agarose gel. Electrophoresis was performed at 80 V for 90 min under refrigeration at 4°C. The AuNP–DNA origami conjugate was then extracted from the agarose gel by centrifugation at 5000 rcf for 10 min at 4°C using a spin filter unit Freeze'N Squeeze; Bio-Rad). Finally, the supernatant was removed, and 50 µl of 1 × TE/Mg buffer was added.

2.4. Preparing Si chip: A Si wafer (Electronics and Materials Corporation) cut into a 10 × 10 mm square was cleaned by sonication in acetone, isopropanol, and UPW (5 min per step). The resulting Si chip was then treated with freshly prepared piranha solution (hydrogen peroxide and sulphuric acid) for 30 min to clean the surface and form silanol groups on the surface. After being rinsed with UPW and isopropanol, the chip was dried with nitrogen. A 3-aminopropyl-triethoxysilane (APTES; Sigma-Aldrich) monolayer, which has a strong positive charge, was then created. This was done by setting the chip in a 120 ml chamber filled with nitrogen and a mixture of 0.2 ml APTES and 1.8 ml toluene. After 2 h reaction at 100°C, the chip was cleaned by sonication in toluene for 10 min and then dried.

2.5. Sacrificial DNA origami technique: Five microlitre of the AuNP–DNA origami solution was applied to the APTES surface of the Si chip and incubated at room temperature. After 30 min, the chip was rinsed with 1 × TE/Mg buffer, 50% ethanol aqueous solution, and 90% ethanol aqueous solution. Finally, the chip was completely dried with nitrogen. A VUV light (Min-Excimer; USHIO) was used to decompose and remove the DNA and APTES layer from the chip. The VUV light had a power of 10 mW/cm$^2$ and was irradiated for 20 min under atmospheric conditions. The distance between the light source and chip surface was set to ∼1 mm. To remove the residue after the VUV irradiation, the chip was dipped in UPW, 90% ethanol aqueous solution, and ethanol for 60 s for each step. Finally, the chip was completely dried with nitrogen.

2.6. FE-SEM imaging: The AuNP–DNA origami conjugates and AuNP dimers fixed on the Si chip were observed with a FE-SEM (SU-8020; Hitachi High-Technologies) operating at 5 kV. All FE-SEM images were obtained with dimensions of 2560 × 1920 pixels and resolution of 2.48 nm/pixel. The contrast of each image was adjusted by analysis software (ImageJ; National Institutes of Health).

2.7. SERS analysis: SERS analyses were performed using a Raman micro-spectroscopic system (LabRAM ARAMIS; Horiba) with a 633 nm wavelength laser and a 2 µm measurement spot size. All experiments were performed with an integration time of 5 s. The decomposition states of the DNA origami and ssDNA covering the AuNP were analysed in air after conjugate deposition, VUV irradiation, and UPW rinsing. To evaluate molecular detection performance, aqueous solutions of 4,4′-bipyridine (TCI Chemicals) with a concentration of 1 mM or 1 µM were used. A silicone rubber sheet 0.5 mm thick with a hole was fixed on the chip under test. An aqueous solution was then dropped into the hole, and then a cover glass was set over the hole to prevent the concentration of 4,4′-bipyridine from increasing due to evaporation of the water.

## 3. Results and discussion

3.1. Evaluating AuNP dimer yield: First, the dependency of the AuNP dimer yield on the number of connector strands on the DNA origami was evaluated. AuNP dimers were prepared from three types of DNA origami with differently installed connector strands (Figs. 2*a*–*c*). The first type (Type-A) had three connectors installed on each face of the partition structure, the second type (Type-B) had six connectors on each face of the partition structure, and the third type (Type-C) had three connectors on each face of the partition structure and three on the base structure at a distance of around 15 nm from the partition structure. Typical FE-SEM images of AuNP–DNA origami conjugates formed using these three types of DNA origami are shown in Figs. 3*a*–*c*. The DNA origami structures were not observed by FE-SEM imaging, but the AuNP spacing within 20 nm, which is twice the maximum length of connector strands, was judged to be connected by DNA origami. The AuNPs in the images were classified as either monomer, dimer, or multimer, as illustrated in Fig. 4. The dimer yields after agarose gel electrophoresis were calculated to be 20% ($N=433$), 17% ($N=451$), and 71% ($N=413$), respectively, for the origami conjugates prepared from DNA origami Types A–C.

For DNA origami Types A and B, which had connector strands only on the partition structure, both AuNP dimer yields were ~20% while it has been reported to be over 50% for rectangular DNA origami [15, 16]. Generally, three connector strands are installed for binding one AuNP, and it should be possible to improve connecting ration by increasing the number of ssDNA connectors due to the stronger binding force [19]. However, in our case, even though the number of ssDNA connectors was increased from three to six, the dimer yield remained about 20%, and no improvement was observed. Therefore, the low AuNP dimer yield was not due to the lack of binding force tightly connecting the AuNPs to the DNA origami.

In contrast, for DNA origami Type-C, which had connector strands on the base structure as well as on the partition structure, the AuNP dimer yield was ~70%. This indicates that the AuNP dimer yield is related to the stiffness of the DNA origami structure in the buffer solution. Since DNA origami consists of dsDNAs that are aligned in parallel and connected to each other, the sheet structure of DNA origami deforms easily along the rows of dsDNAs [20, 21]. As shown in Fig. 5*a*, when one AuNP was connected to the partition structure on one side, the approach of another AuNP to the opposite face was blocked by the deformation of the DNA origami due to electrostatic repulsion between the AuNP already connected and the base structure of the DNA origami. In contrast,

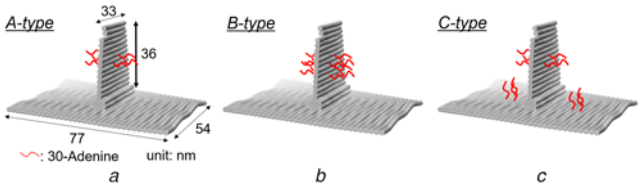


**Fig. 2** *Schematic illustrations of DNA origami*
*a* Three connectors on partition structure (A-type)
*b* Six connectors on partition structure (B-type)
*c* Three connectors on both partition and base structure (C-type)

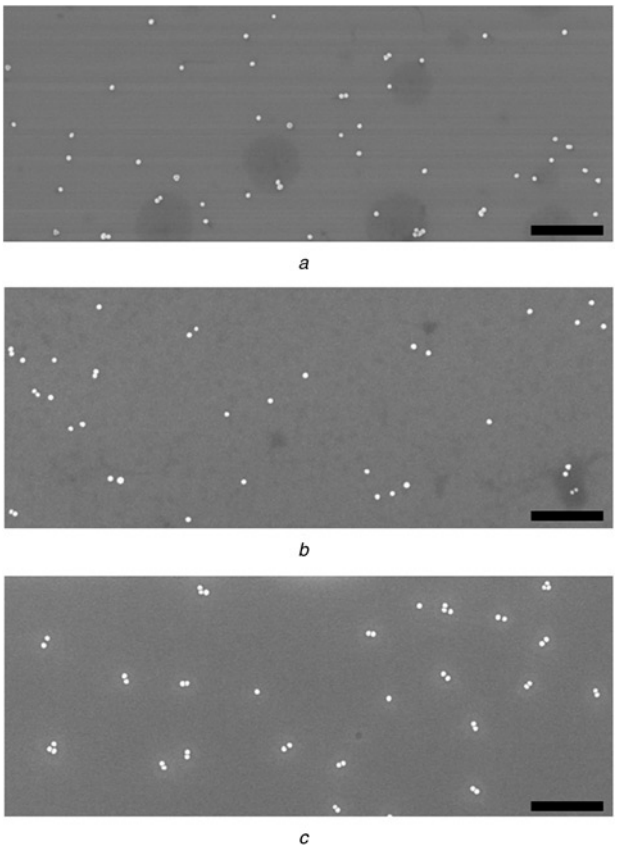


**Fig. 3** *FE-SEM images of AuNP-DNA origami conjugates*
*a* Formed with A-type DNA origami
*b* B-type DNA origami
*c* C-type DNA origami (scale bar: 500 nm)

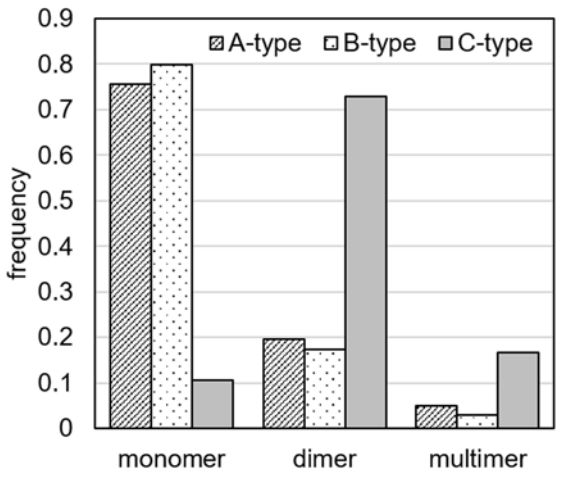


**Fig. 4** *Classification of AuNPs in FE-SEM images of origami conjugates formed with three types of DNA origami*

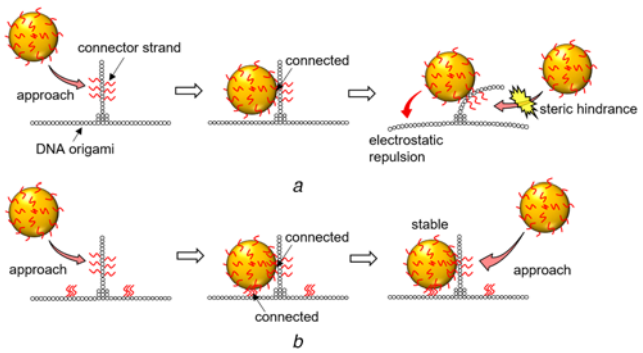


**Fig. 5** *Schematic illustrations of DNA origami deformation in solution during conjugate creation*
*a* A-type and B-type
*b* C-type




doi: 10.1049/mnl.2019.0416

as shown in Fig. 5*b*, when connector strands were additionally installed on the base structure, the deformation of the DNA origami was suppressed since the partition structure was tightly fixed to the base structure via the AuNP. Thus, the connector strands on the opposite face of the partition structure were not hidden, and the AuNP connection rate was greatly improved. Given these results, DNA origami with connector ssDNA on both the partition and base structure were used for the following experiments.

3.2. Evaluating state of decomposing DNA origami: An FE-SEM image of the Si substrate used in this experiment is shown in Fig. 6. The average density of the well-formed AuNP–DNA origami conjugates on the Si substrate was evaluated from such images, and the average quantity in the 2 μm measurement laser spot was calculated to be 1.5. However, since the AuNP–DNA origami conjugates were randomly deposited on the Si substrate, the quantity greatly depended on the measurement area. The maximum number of dimers contained in the laser diameter in the SERS analysis was around five. The state of the decomposing DNA origami was evaluated by SERS analysis in air after each phase of the cleaning process of the sacrificial DNA origami technique.

Figs. 7*a–c* show typical SERS spectra obtained after adsorption of the conjugates on a Si chip, VUV irradiation, and UPW rinsing, respectively. Each graph shows five representative measurement results obtained for different measurement locations. The signal observed around 900–1000 $cm^{-1}$ was from the Si used as a substrate. Since the AuNP–DNA origami conjugates were randomly adsorbed on the substrate, the angle of laser polarisation and the long axis of the AuNP dimers, which is important for SERS analysis to obtain strong signal enhancement, were mismatched. Hence, the AuNP dimers in many measurement locations did not contribute to the SERS signal of the residual DNA origami, and only the Raman signal from the Si chip was detected.

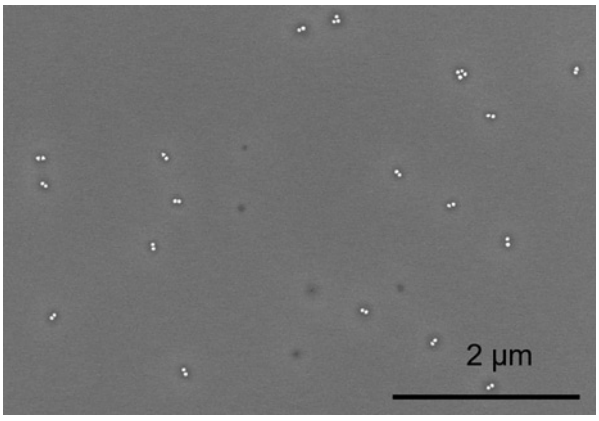


**Fig. 6** *FE-SEM image of Si chip used in SERS analyses in air (scale bar: 2 μm)*

In the conjugate adsorption phase, SERS signals from the DNA were detected, but they were not clear since large broad peaks were mainly detected at ∼1350 and ∼1600 $cm^{-1}$, as shown in Fig. 7*a*. These peaks correspond to the D band and G band, respectively, of graphite and indicate carbonisation of the DNA origami due to the high temperature generated in the nanogaps by the laser irradiation used for measurement in this analysis [22, 23]. In the results after VUV irradiation (Fig. 7*b*), the signals at ∼1350 and ∼1600 $cm^{-1}$ were weak compared with those after conjugate adsorption (Fig. 7*a*). This clearly shows that the DNA origami were decomposed and that the absolute number of DNA molecules in the nanogaps decreased due to both the cleaning effect of the irradiated VUV and the simultaneously generated active oxygen. However, SERS signals from the phosphorus of the DNA backbone and DNA bases, which indicates the existence of residual DNA origami not completely decomposed even after VUV irradiation, were also detected. In the measurement after UPW rinsing (Fig. 7*c*), only the signal from the Si substrate was observed at every measured location. The DNA fragments remaining after VUV irradiation had been completely removed by the UPW rinsing. These results indicate that complete DNA removal is achieved by the cleaning process of the sacrificial DNA origami technique and that surface-clean AuNP dimers, which are useful for sensitive molecular trace analysis with SERS without generating noise from DNA, were successfully formed.

3.3. Evaluating the performance of molecular detection: Molecular trace analyses from 1 mM and 1 μM 4,4′-bipyridine aqueous solutions were performed using a substrate with AuNP dimers formed using the sacrificial DNA origami technique. The molecular structure of the 4,4′-bipyridine is shown in Fig. 8. The 4,4′-bipyridine molecule consists of two pyridines, each with a nitrogen atom at the 4-position, and the distance between the two nitrogen atoms is about 0.7 nm [24]. The SERS signals from

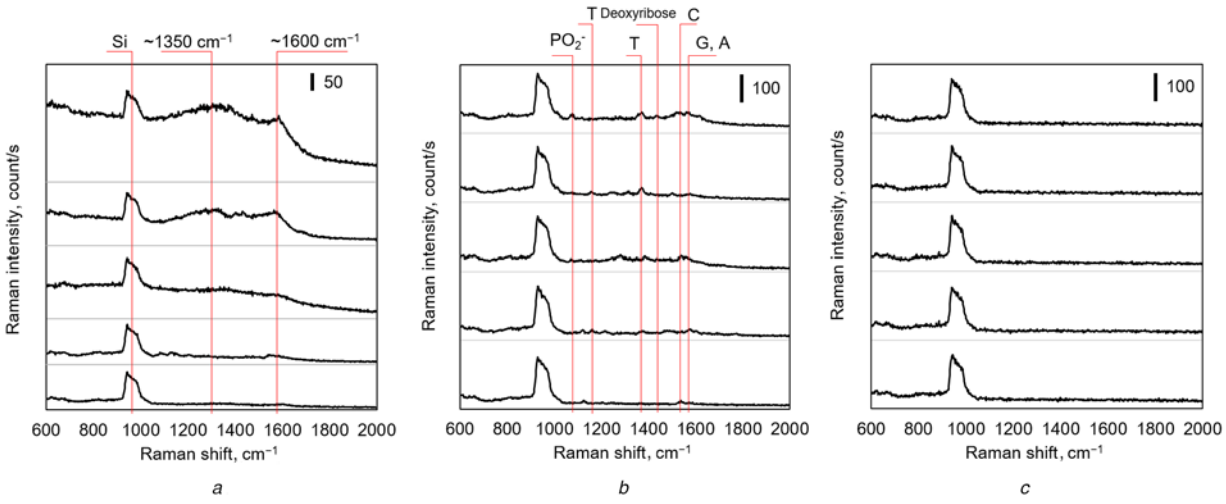


**Fig. 7** *Results of SERS analyses in air obtained for different measurement locations*
*a* After conjugate deposition
*b* VUV irradiation
*c* UPW rinsing

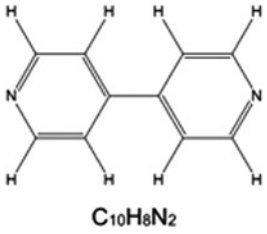


**Fig. 8** *Molecular structure of 4,4′-bipyridine*

4,4′-bipyridine adsorbing to AuNPs measured in another study are shown in Table 1 [25].

An FE-SEM image of the Si substrate used is shown in Fig. 9. The average number of AuNP dimers in a 2 μm laser spot was calculated to be 3.1 from this image. The results of molecular trace analysis using 4,4′-bipyridine aqueous solution with concentrations of 1 mM and 1 μM are shown in Figs. 10*a* and *b*, respectively. Each graph shows four representative results obtained for the different measurement locations on the substrate. For comparison, the spectrum obtained from a substrate with well-dispersed AuNP monomers (average of 19.9 in 2 μm laser spot) that was prepared by depositing ssDNA–AuNPs and then applying the sacrificial DNA origami technique is plotted at the bottom by the black line. These results show that some or all of the SERS signals from the 4,4′-bipyridine (Table 1) were enhanced and detected when AuNP dimers were present in the measurement laser spot while Raman signals of 4,4′-bipyridine were not detected from the substrate, which did not have AuNP dimers.

In the SERS spectra detected from the 1 mM aqueous solution, all 4,4′-bipyridine signals were detected, and the signals at Raman shifts of 1017, 1227, 1293, and 1608 $cm^{-1}$ were particularly strong, similar to the results of other research [1, 25]. On the other hand, with the 1 μM aqueous solution, the same four signals were mainly detected while other relatively weak signals were below the noise level and were not detected.

**Table 1** SERS spectrum of 4,4′-bipyridine [25]

| Raman shift, $cm^{-1}$ | Assignment |
|---|---|
| 766 | ring in-plane deformation |
| 856 | ring breath |
| 1017 | CH out-of-plane bend |
| 1080 | ring in-plane deformation + CH bend |
| 1227 | CH in-plane bend |
| 1293 | inter-ring stretch |
| 1510 | CH in-plane bend + ring stretch |
| 1608 | ring stretch |

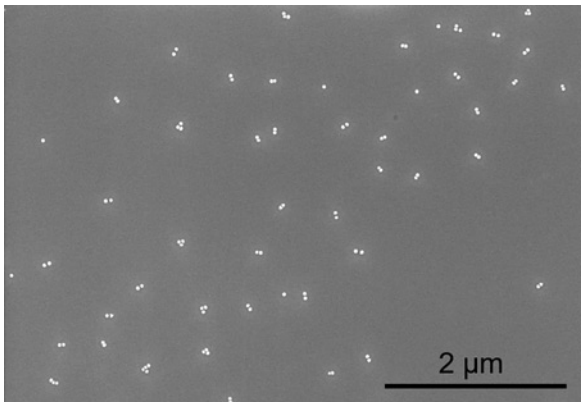


**Fig. 9** *FE-SEM image of silicon chip used in SERS analysis for molecular detection (scale bar: 2 μm)*

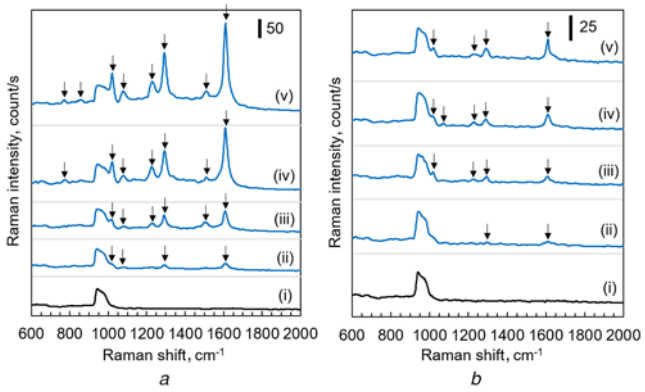


**Fig. 10** *Results of SERS analysis*
*a* 1 mM aqueous solution
*b* 1 μM aqueous solution
(i) Obtained from silicon chip with AuNP monomers; (ii)–(v) obtained from different measurement locations on Si chip with randomly deposited AuNP dimers (arrows indicate detected signals listed in Table 1.)

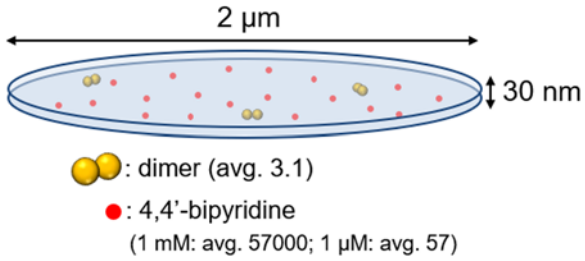


**Fig. 11** *Schematic model of molecular detection experiment*

A possible reason for the difference in signal intensity between the solutions was the quantity of target molecules adsorbed in the nanogaps. The schematic illustration of this experiment is shown in Fig. 11. In a cylinder with a 2 μm diameter and 30 nm height representing the measurement area, the quantity of AuNP dimers was 3.1 on average, and the quantities of 4,4′-bipyridine in 1 mM and 1 μM aqueous solution were calculated to be 57,000 and 57. For the 1 mM solution, several molecules should be able to adsorb into the nanogaps and generate SERS signals given the relatively high molecular concentration in the cylinder and the 0.7 nm size of the 4,4′-bipyridine. On the other hand, for the 1 μM solution, the amount of 4,4′-bipyridine adsorption in the nanogaps should be only 0 or 1 due to the low molecular concentration in the cylinder. Therefore, the signal intensities of the 4,4′-bipyridine were weaker when the molecular concentration was lower while the major signals of 4,4′- bipyridine were successfully detected even for a 1 μM solution.

Although the signal intensity varied depending on the measurement location, signal from 4,4′-bipyridine was successfully detected from a low concentration aqueous solution with an average of 3.1 AuNP dimers per measurement location. This indicates that AuNP dimers formed using the sacrificial DNA origami technique have high sensitivity at the level of single-molecule detection in SERS analysis.

**4. Conclusion:** This research was conducted with the aim of evaluating the performance of AuNP dimers formed using a sacrificial DNA origami technique for molecular detection based on SERS. To evaluate its performance, AuNPs with a diameter of 30 nm




doi: 10.1049/mnl.2019.0416

were connected to the counter-face of DNA origami structures, and a 70% dimer yield was successfully obtained by improving structure stiffness in buffer solution. SERS analysis in air performed after cleaning demonstrated that the combination of VUV irradiation and UPW rinsing can completely remove DNA origami between AuNPs in a pair. The AuNP dimers enhanced the Raman signals of the 4,4′-bipyridine used as a target in molecular trace analysis. These results demonstrate the feasibility of highly sensitive SERS-based molecular detection with AuNP dimers formed using the sacrificial DNA origami technique.

**5. Acknowledgments:** This project was supported by a Japan Society for the Promotion of Science Grant-in-Aid for Scientific Research B (grant no. 16H03841) and partly supported by the Kyoto Integrated Science and Technology Bio-Analysis Center, Japan.

## 6 References

[1] Sugano K.: 'Single molecule SERS with directionally arrayed gold nanoparticle dimers on substrate', *ECS Trans.*, 2016, **75**, (17), pp. 3–10

[2] Sugano K., Ikegami K., Isono Y.: 'Characterization method for relative Raman enhancement for surface-enhanced Raman spectroscopy using gold nanoparticle dimer array', *Jpn J. Appl. Phys.*, 2017, **56**, (6S1), pp. 1–6

[3] Sugano K., Matsui D., Tsuchiya T, *ET AL.*: 'Ultrasensitive surface-enhanced Raman spectroscopy using directionally arrayed gold nanoparticle dimers'. 2015 28th IEEE Int. Conf. on Micro Electro Mechanical Systems (MEMS), Estoril, Portugal, 18–22 Jan. 2015, pp. 608–611

[4] Gopinath A., Boriskina S. V., Reinhard B.M., *ET AL.*: 'Deterministic aperiodic arrays of metal nanoparticles for surface-enhanced Raman scattering (SERS)', *Opt. Express*, 2009, **17**, (5), pp. 3741–3753.A

[5] Haes A.J., Haynes C.L., McFarland A.D., *ET AL.*: 'Plasmonic materials for surface-enhanced sensing and spectroscopy', *MRS Bull.*, 2005, **30**, (5), pp. 368–375

[6] Sun Q., Ueno K., Yu H., *ET AL.*: 'Direct imaging of the near field and dynamics of surface plasmon resonance on gold nanostructures using photoemission electron microscopy', *Light, Sci. Appl.*, 2013, **2**, (12), p. e118

[7] Félidj N., Truong S.L., Aubard J., *ET AL.*: 'Gold particle interaction in regular arrays probed by surface enhanced Raman scattering', *J. Chem. Phys.*, 2004, **120**, (15), pp. 7141–7146

[8] Milekhin A.G., Sveshnikova L.L., Duda T.A., *ET AL.*: 'Resonant surface-enhanced Raman scattering by optical phonons in a monolayer of CdSe nanocrystals on Au nanocluster arrays', *Appl. Surface Sci.*, 2016, **370**, pp. 410–417

[9] Cui Y., Björk M.T., Liddle J.A., *ET AL.*: 'Integration of colloidal nanocrystals into lithographically patterned devices', *Nano Lett.*, 2004, **4**, (6), pp. 1093–1098

[10] Alexander K.D., Hampton M.J., Zhang S., *ET AL.*: 'A high-throughput method for controlled hot-spot fabrication in SERS-active gold nanoparticle dimer arrays', *J. Raman Spectrosc.*, 2009, **40**, (12), pp. 2171–2175

[11] Thacker V.V., Herrmann L.O., Sigle D.O., *ET AL.*: 'DNA origami based assembly of gold nanoparticle dimers for surface-enhanced Raman scattering', *Nat. Commun.*, 2014, **5**, pp. 1–7

[12] Zhao M., Wang X., Ren S., *ET AL.*: 'Cavity-type DNA origami-based plasmonic nanostructures for Raman enhancement', *ACS Appl. Mater. Interfaces*, 2017, **9**, (26), pp. 21942–21948

[13] Prinz J., Schreiber B., Olejko L., *ET AL.*: 'DNA origami substrates for highly sensitive surface-enhanced Raman scattering', *J. Phys. Chem. Lett.*, 2013, **4**, (23), pp. 4140–4145

[14] Heck C., Prinz J., Dathe A., *ET AL.*: 'Gold nanolenses self-assembled by DNA origami', *ACS Photonics*, 2017, **4**, (5), pp. 1123–1130

[15] Simoncelli S., Roller E. M., Urban P., *ET AL.*: 'Quantitative single-molecule surface-enhanced Raman scattering by optothermal tuning of DNA origami-assembled plasmonic nanoantennas', *ACS Nano*, 2016, **10**, (11), pp. 9809–9815

[16] Kühler P., Roller E.M., Schreiber R., *ET AL.*: 'Plasmonic DNA-origami nanoantennas for surface-enhanced Raman spectroscopy', *Nano Lett.*, 2014, **14**, (5), pp. 2914–2919

[17] Rothemund P.W.K.: 'Folding DNA to create nanoscale shapes and patterns', *Nature*, 2006, **440**, (7082), pp. 297–302

[18] Yamashita N., Ma Z., Park, *ET AL.*: 'Formation of gold nanoparticle dimers on silicon by sacrificial DNA origami technique', *Micro Nano Lett.*, 2017, **12**, (11), pp. 854–859

[19] Prinz J., Heck C., Ellerik L., *ET AL.*: 'DNA origami based Au-Ag-core-shell nanoparticle dimers with single-molecule SERS sensitivity', *Nanoscale*, 2016, **8**, (10), pp. 5612–5620

[20] Shen X., Song C., Wang J., *ET AL.*: 'Rolling up gold nanoparticle-dressed DNA origami into three-dimensional plasmonic chiral nanostructures', *J. Am. Chem. Soc.*, 2011, **134**, (1), pp. 146–149

[21] Fu Y., Zeng D., Chao J., *ET AL.*: 'Single-step rapid assembly of DNA origami nanostructures for addressable nanoscale bioreactors', *J. Am. Chem. Soc.*, 2012, **135**, (2), pp. 696–702

[22] Stehr J., Hrelescu C., Sperling R. A., *ET AL.*: 'Gold nanostoves for microsecond DNA melting analysis', *Nano Lett.*, 2008, **8**, (2), pp. 619–623

[23] Nakao H., Tokonami S., Yamamoto Y., *ET AL.*: 'Fluorescent carbon nanowires made by pyrolysis of DNA nanofibers and plasmon-assisted emission enhancement of their fluorescence', *Chem. Commun.*, 2014, **50**, (80), pp. 11887–11890

[24] Bâldea I.: 'Floppy molecules as candidates for achieving opto-electronic molecular devices without skeletal rearrangement or bond breaking', *Phys. Chem. Chem. Phys.*, 2017, **19**, (45), pp. 30842–30851

[25] Suzuki M., Niidome Y., Yamada S.: 'Adsorption characteristics of 4,4′-bipyridine molecules on gold nanosphere films studied by surface-enhanced Raman scattering', *Thin Solid Films*, 2006, **496**, (2), pp. 740–747